Mn 3d states in NiAs-type MnTe studied by means of synchrotron radiation photoemission

Mn 3d states in NiAs-type MnTe studied by means of synchrotron radiation photoemission

Y Ueda†§, H Sato†, M Taniguchi†, N Happo†, T Mihara†, H Namatame†, T Mizokawa‡ and A Fujimori‡

† Department of Materials Science, Faculty of Science, Hiroshima University, Kagamiyama 1-3, Higashi-Hiroshima 724, Japan
‡ Department of Physics, The University of Tokyo, Bunkyo-ku, Tokyo 113, Japan

Abstract. A measure of the Mn 3d partial density of states (DOS) of NiAs-type MnTe has been obtained from resonant photoemission experiments in the Mn 3p–3d core excitation region. On the basis of an analysis of the Mn 3d partial DOS spectrum in terms of a configuration interaction on a Mn^{2+} $(Te^{2-})_6$ model cluster, we find that the spectral intensities in the top 6 eV are predominantly due to transitions to the $d^5\underline{L}$ final-state configuration, where $\underline{L}$ represents a ligand hole. On the other hand, those at 6–14 eV originate mainly from transitions to the d^4 configuration.

Among transition-metal compounds with hexagonal NiAs-type structure, MnTe is a particularly interesting material because of its non-standard magnetic and electronic behaviour [1–3]. Most of the materials belonging to this group are metallic or semimetallic, while MnTe is a semiconductor with a direct band-gap energy of 1.3 eV [4]. The other manganese chalcogenides (MnO, MnS and MnSe) are wide-gap insulators and their stable structure is NaCl type [4–6]. Therefore, semiconducting MnTe occupies an intermediate position between NiAs-type metallic transition-metal compounds and NaCl-type insulating manganese chalcogenides. With respect to the magnetic properties of NiAs-type MnTe, it is well known that the crystal is antiferromagnetic with a Néel temperature T_N of 307 K [7]. A number of studies have been made using neutron diffraction [8], pressure-induced phase transitions [9], optical absorption [4, 10, 11], x-ray photoemission measurements [12] and band-structure calculations [13–16] so far.

The purpose of the present paper is to evaluate a measure of the Mn 3d-derived partial density of states (DOS) of NiAs-type MnTe in the valence bands and to investigate the degree of hybridization in detail from resonant photoemission measurements in the Mn 3p–3d core excitation region [17–19]. The resonance takes place over a specific energy range as a result of interference between the direct excitation process of the Mn 3d electrons ($3p^63d^5 + \hbar\omega \rightarrow 3p^63d^4 + \epsilon l$) and the discrete Mn 3p–3d excitation process followed by a super Coster–Kronig decay ($3p^63d^5 + \hbar\omega \rightarrow 3p^53d^6 \rightarrow 3p^63d^4 + \epsilon l$), where $\hbar\omega$ is the excitation photon energy [20]. Since only the Mn 3d states are resonantly enhanced for $\hbar\omega$ near the Mn 3p–3d excitation, we can estimate their contribution to the valence band DOS by subtracting the spectrum at antiresonance from that measured just on resonance. The

§ Present address: Tokuyama National College of Technology, Kume Takajo 3538, Tokuyama 745, Japan.

cross sections of the remaining states (Te 5s and 5p) do not vary appreciably over the small energy region of the resonance.

Total yield and valence band photoemission measurements were carried out with the aid of synchrotron radiation on the beamline 11D of the Photon Factory in the National Laboratory for High Energy Physics (KEK-PF). Total yield mode was employed to obtain core absorption spectra. In addition, a combination of a constant-deviation-type monochromator and a double-stage cylindrical-mirror analyser was used to measure angle-integrated photoemission spectra. The binding energy with respect to the valence band maximum (VBM) was determined by extrapolating the steep leading edge of the highest valence band peak to the baseline. The intensities of the total yield spectra and valence band spectra for resonant photoemission experiments were normalized to the monochromator output.

The background due to inelastic secondary electrons in the valence band spectra were, in some cases, removed from the spectra. Then, we assumed that the intensity $I_s(E)$ of secondary electrons at a binding energy E is given by

$$I_s(E) = k \int_{E_0}^{E} I(E') \, dE' \tag{1}$$

where $I(E')$, E_0 and k represent the total emission intensity at binding energy E', the binding energy corresponding to the highest kinetic energy of emitted electrons and a constant, respectively [21]. The constant k can be determined by applying (1) to the emission intensity at binding energy E_a where the entire contribution is only from secondary electrons. Then, k satisfies the following relation

$$k = I_s(E_a) \Big/ \int_{E_0}^{E_a} I(E') \, dE'. \tag{2}$$

The working pressure in the analysis chamber was 4×10^{-10} Torr during the measurements. All measurements were performed at room temperature.

Polycrystals of NiAs-type MnTe were grown by quenching the quartz ampoule with equal amounts of Mn and Te from 1000 °C to room temperature [22]. A small amount of Na (below 0.1 at.%) was doped into the crystals [23] to realize a low resistivity and to prevent the electrostatic charging effect in photoemission measurements. The crystal structure was checked by x-ray diffraction measurements. The Mn and Te concentration were evaluated by electron probe microanalysis. Clean surfaces for photoemission measurements were obtained by scraping with a diamond file under 4×10^{-10} Torr.

Figure 1 shows a series of valence band spectra of NiAs-type MnTe for $\hbar\omega$ in the Mn 3p–3d core excitation region. The intensities have been normalized to the monochromator output; thus the spectra can be compared not only with respect to their shape but also in terms of relative intensities. One notices six structures at 0.6, 2.4, 3.7, 5.0, about 8.0 and 11.5 eV below the VBM as shown by vertical arrows for the spectra taken at $\hbar\omega = 47.4$ and 50.0 eV. Among these structures, the peak at 3.7 eV exhibits a prominent resonance. With increasing $\hbar\omega$ from 43.0 to 60.0 eV, the intensity of this peak first decreases gradually to a minimum at $\hbar\omega = 47.4$ eV and then increases sharply to reach a maximum at $\hbar\omega = 50.0$ eV. The remainder of the valence bands are also resonantly enhanced. In particular, a set of states appears between 6 and 14 eV near the resonance.

In order to investigate the resonant profile in detail, we plot the photoemission intensities of selected valence band features as a function of $\hbar\omega$ in figure 2(a), where each valence
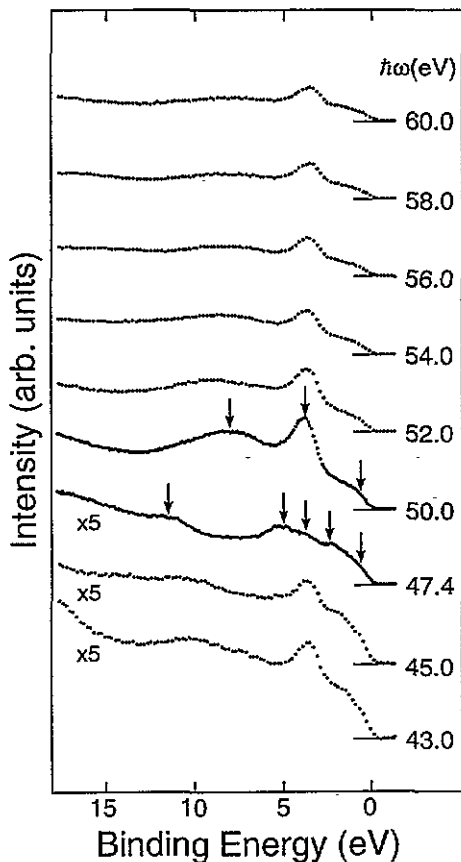
Figure 1. A series of valence band photoemission spectra of NiAs-type MnTe for $\hbar\omega$ in the Mn 3p–3d excitation region. The binding energy is defined relative to the VBM. The vertical arrows represent energy positions of structures.

band is specified by the binding energy E_i with respect to the VBM. One notices that the spectrum for $E_i = 3.8$ eV shows a prominent Fano-type resonance [20, 24]. In addition, the spectra for $E_i = 1.0$ and 2.1 eV also exhibit resonance. The amount of enhancement for the spectrum for $E_i = 1.0$ eV is as much as about quarter of that for the spectrum for $E_i = 3.8$ eV. As far as the spectra for $E_i = 5.5$ and 8.1 eV are concerned, these spectra are affected by the background of inelastic secondary electrons. After correction for the background contribution, however, we still obtain a sizable resonance. The correlation of the valence band resonance with the Mn 3p–3d core excitation is clear from comparison with the corresponding absorption spectrum of MnTe in figure 2(b), obtained in the form of the total yield spectrum.

Here, we realize our aim to deduce a measure of the Mn 3d partial DOS of MnTe. For this purpose, we subtract the spectrum measured at antiresonance ($\hbar\omega = 47.4$ eV) from that taken just on resonance ($\hbar\omega = 50.0$ eV), after normalization of the spectral intensities to the monochromator output. The result is shown in figure 3(a). We find a prominant peak again at 3.7 eV, and an appreciable Mn 3d contribution throughout the valence bands from 0 to 6 eV. In addition, the difference spectrum shows a satellite structure in the energy region from 6 to 14 eV.
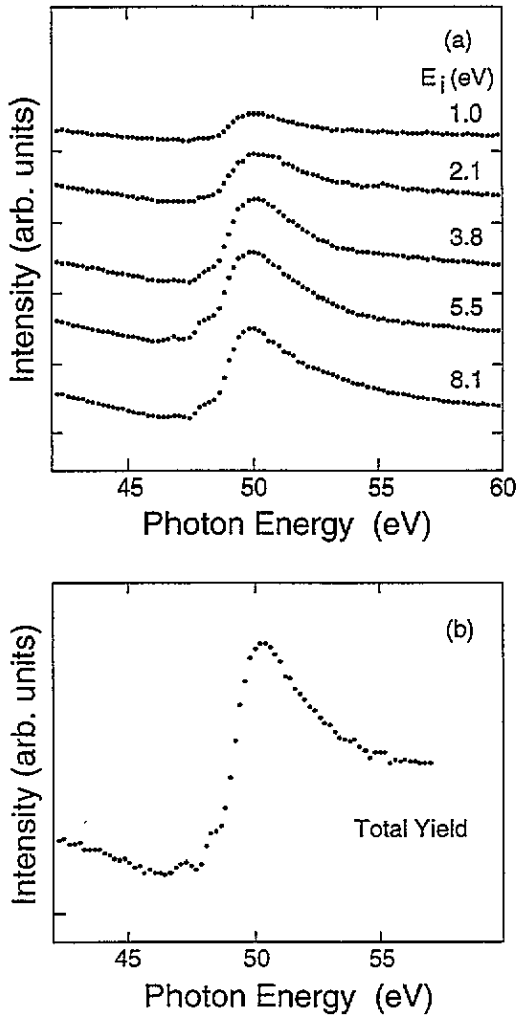
Figure 2. (a) Plots of the photoemission intensities of selected valence bands as a function of $\hbar\omega$. Each valence band is specified by the binding energy E_l with respect to the VBM. (b) Total yield spectrum of NiAs-type MnTe for the photon energy region between 40 and 57 eV.

In order to analyse the Mn 3d partial DOS features in detail, we have performed a configuration interaction (CI) calculation on a model cluster Mn^{2+} $(Te^{2-})_6$, following similar calculations for $Cd_{1-x}Mn_xTe$ alloys [17, 18, 25]. In the calculation, the ground state is represented as a mixture of the purely ionic d^5 configuration and the charge-transfer configurations of $d^6\underline{L}$ and $d^7\underline{L}^2$:

$$\Psi_g = a_g|d^5\rangle + b_g|d^6\underline{L}\rangle + c_g|d^7\underline{L}^2\rangle \tag{3}$$

where $\underline{L}$ denotes a ligand hole. The final state of d-electron emission is a mixture of the d^4, $d^5\underline{L}$ and $d^6\underline{L}^2$ configurations as given by

$$\Psi_f = a_f|d^4\rangle + b_f|d^5\underline{L}\rangle + c_f|d^6\underline{L}^2\rangle. \tag{4}$$
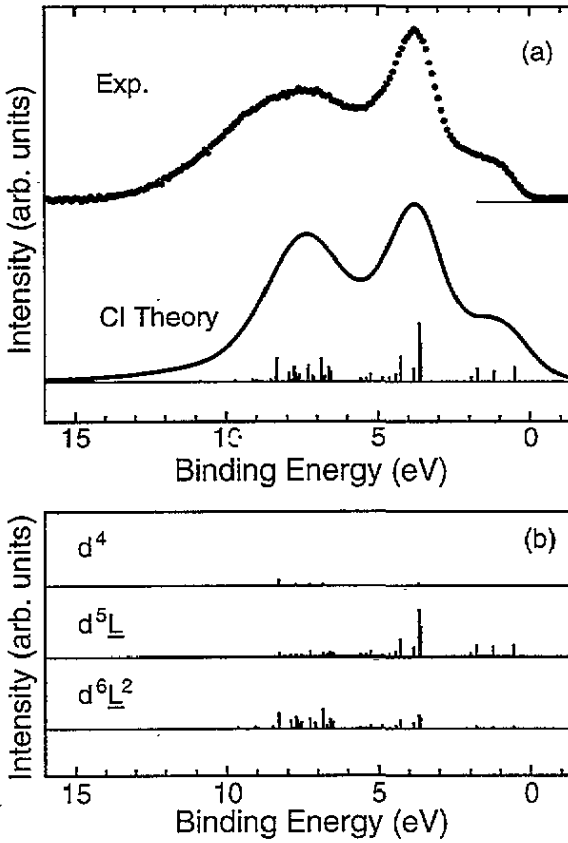
Figure 3. (a) A comparison between the experimental Mn 3d partial DOS spectrum and model spectrum calculated in terms of the CI theory using parameters of $\Delta = 2.0$ eV, $U = 5.0$ eV and $(pd\sigma) = -0.75$ eV. (b) Final states decomposed into the d^4, $d^5\underline{L}$ and $d^6\underline{L}^2$ components.

The $d^5\underline{L}$ configuration, for instance, originates from the screening of the photoproduced hole in the Mn 3d states by a ligand-to-metal charge transfer as well as from direct d-electron emission from the $d^6\underline{L}$ component in equation (3).

The calculated Mn 3d DOS spectrum is shown in figure 3(a), where the line spectra are convoluted with Gaussian and Lorentzian functions for comparison with the experimental spectrum [26, 27]. We find that the experimental spectrum is well reproduced using the parameters $\Delta = 2.0$ eV, $U = 5.0$ eV and $(pd\sigma) = -0.75$ eV, where Δ is ligand-to-metal charge-transfer energy and U is Coulomb correlation energy of Mn 3d electrons. $(pd\sigma)$ denotes a p–d transfer integral and $(pd\sigma)/(pd\pi)$ is fixed at -2.16 [28]. In figure 3(b), the final state is decomposed into the d^4, $d^5\underline{L}$ and $d^6\underline{L}^2$ components.

The present CI analysis reveals that the intensities of the line spectra in the top 6 eV (figure 3(a)) originate predominantly from transitions into the $d^5\underline{L}$ final-state configuration with a smaller contribution of the d^4 configuration. On the other hand, those at 6–14 eV stem mainly from transitions into the d^4 configuration, while the transitions into the $d^5\underline{L}$ configuration contribute to a lesser extent.

Finally, we comment on the theoretical valence band DOS of NiAs-type MnTe calculated by Wei and Zunger [16] on the basis of the spin-polarized self-consistent local-spin-

density total-energy and band-structure calculation. The theoretical DOS of valence bands is composed of the Te 5s bands centred at 11.8 eV with a band width of 1.5 eV, and the upper Te 5p and Mn 3d hybridization bands in the energy region from 0 to 6 eV. The characteristic feature of the theoretical DOS is qualitatively consistent with the experimental spectrum measured at 47.4 eV. We find that the spectra in figure 2(a) can be roughly reproduced using a Fano profile with q-parameters of around 2. For such q-values, the Mn 3d cross section in the 1–14 eV range is nearly zero at antiresonance [20, 24]. Therefore, the spectrum at 47.4 eV can be reasonably assumed to reflect predominantly information on the sp-band states.

Acknowledgments

References

[1] Kjekshus A and Pearson W B 1964 *Progress in Solid State Chemistry* vol 1, ed H Reiss (Oxford: Pergamon) p 83
[2] Motizuki K and Katoh K 1984 *J. Phys. Soc. Japan* **53** 735
[3] Neizel U and Bärner K 1985 *Phys. Status Solidi* b **129** 707
[4] Allen J W, Lucovsky G and Mikkelsen J C Jr 1977 *Solid State Commun.* **24** 367
[5] Decker D L and Wild R L 1971 *Phys. Rev.* **4** 3425
[6] Oguchi T, Terakura K and Williams A R 1983 *Phys. Rev.* B **28** 6443
[7] Ozawa K, Anzai S and Hamaguchi Y 1966 *Phys. Rev.* **20** 132
[8] Kunitomi N, Hamaguchi Y and Anzai S 1964 *J. Physique* **25** 568
[9] Mimasa M, Sakamoto I, Murata K, Fujii Y and Onodera A 1987 *J. Phys. C: Solid State Phys.* **20** 4689
[10] Zviagin A I, Povstianyi L A and Arefieva P M 1971 *Izv. Akad. Nauk SSSR* **35** 1190
[11] Onari S, Arai T and Kudo K 1974 *Solid State Commun.* **14** 507
[12] Franzen H and Sterner C 1978 *J. Solid State Chem.* **25** 227
[13] Sandratskii L M, Egorov R F and Bedryshev A A 1981 *Phys. Status Solidi* b **140** 103
[14] Podgòrny M nad Oeskiewicz J 1983 *J. Phys. C: Solid State Phys.* **16** 2547
[15] Mašek, Vellický B and Janiš V 1987 *J. Phys. C: Solid State Phys.* **20** 59
[16] Wei S-H and Zunger A 1987 *Phys. Rev.* B **35** 2340
[17] Ley L, Taniguchi M, Ghijsen J and Johnson R L 1987 *Phys. Rev.* B **35** 2839
[18] Taniguchi M, Ley L, Johnson R L, Ghijsen J and Cardona M 1986 *Phys. Rev.* B **33** 1206
[19] Fujimori A, Saeki M, Kimizuka N, Taniguchi M and Suga S 1986 *Phys. Rev.* B **34** 7318
[20] Kotani A and Toyozawa Y 1979 *Synchrotron Radiation* ed C Kunz (Berlin: Springer) p 169
[21] Shirley D A 1972 *Phys. Rev.* B **5** 4709
[22] Matcika D 1972 *J. Cryst. Growth* **13–14** 698
[23] Zanmarchi G 1967 *J. Phys. Chem. Solids* **28** 2123
[24] Fano U 1961 *Phys. Rev.* **124** 1866
[25] Fujimori A and Mizokawa T 1993 *II–VI Semiconductor Compounds* ed M Jain (Singapore: World Scientific) p 103
[26] Fujimori A and Minami A 1984 *Phys. Rev.* B **30** 957
[27] Line spectra are convoluted with a Gaussian of 0.83 eV full width at half-maximum and a Lorentian function, the width of which are scaled with the binding energy E eV as $0.1E$, according to the procedure in [26]
[28] Harrison W A 1980 *Electronic Structure and the Properties of Solids* (San Francisco, CA: Freeman) p 451